Grey balance adjusting in image processing using gradation trajectories

Oleg B. Milder[1] and Dmitry A. Tarasov[1,2]

[1] Ural Federal University, Institute of Radio-Engineering and IT, Mira, 32, Ekaterinburg 620002 RUSSIA
[2] Institute of Industrial Ecology UB RAS, Kovalevskoy, 20, Ekaterinburg 620990 RUSSIA
datarasov@yandex.ru

Abstract. Grey balance adjusting is one of the key moments in digital image processing. In the work, an experimental attempt was made to adapt the ideas about the Maxwell color triangle (additive color synthesis) to the patterns of autotypic color synthesis. To adjust the grey balance, it is suggested not to use colorants of autotypic synthesis (CMYK), but their double overlays (RGB). As double overlays, it is proposed to use geodesic lines on the gradation surfaces of the corresponding double overlays. All geometric objects (points, lines, and surfaces) are considered in the CIE *Lab* space. The metric of the space is determined by the magnitude of the color difference CIE *dE*. Experimental verification of the approach and discussion of the results were carried out.

Keywords: Geodesics, gradation trajectories, grey balance, image processing

1 Introduction

Grey balance is the basic and substantial control parameter in image processing, which operates by balancing the correlation of substrate features and print control parameters. The grey balance together with different color prediction models (CPMs) helps users to adjust colors in print and improve the color management. Another benefit of well-grey-balanced printing system is shortage of ink usage that is particularly important in the case of current multi-colors printers. Today, there are many CPMs. Such models take a set of inks as inputs and predict the resulting color in print, as specified by reflectance or tristimulus values.

Empirical surface color prediction models take into account superposition of ink halftones and do not deal with the light propagation and fading within the print. The models demonstrate the relationship between reflected light and surface coverages by colorants. Physically inspired models engage a more detailed analysis of light-print interaction based on the mathematical prediction of how the light paths go within a halftone print and what the resulting fade is. Ink spreading models characterize the effective surface of an ink dot after

it has been printed at a given nominal surface coverage compared to the effective surface coverage that forms the physical dot gain. The models accounting the ink spreading in all ink superposition conditions rely on the ink spreading curves. The curves map the nominal surface coverages to effective surface coverages for the surface coverages of single ink halftones and ones superposed with one and two solid inks. The further development of the color prediction models deal with spread-based light propagation and transportation probability. Spectral reflection prediction models study the impact of different factors influencing the range of printable colors (the inks, substrate, illumination conditions, and halftones) and create the printer characterization profiles for the purpose of color management [1]. These models together with the ink-spreading models take into account physical dot gain and are able to predict the reflectance spectra as a function of ink surface coverage for 2–4 inks (binary and ternary color systems). The models uses multiple tone reproduction (ink spreading) curves (TRC) to characterize the physical dot gain of the ink halftones on the substrate and in all solid ink superposition conditions [2–4]. Different color prediction models have been successfully applied to color reproduction management in various contexts [5–9]. The major drawback of the mentioned models is the fact that all of them are computationally capacious, as n colorants require a solution of system of 2^n equations; therefore, they cannot be implicated into real workflow.

The empirical approaches are more promising; however, they usually require a significant amount of print tests to do. Most practitioners prefer using relatively simple methods for setting up printing systems by analyzing gradation scales and applying the gradation-based techniques that are known as an indispensable attribute of color printing systems settings [10, pp. 88–89]. At the same time, we express doubts about the rational use of these characteristics in the digital printing technology. The main problem is in the fact that using the gradation curves in conventional 2D embodiment significantly reduces the quantity and quality of information extracted from them. In work [11], the 3D gradation trajectories are introduced as a further development of the gradation curves approach. Implication of the mathematical apparatus of differential geometry for gradation trajectories analysis in 3D CIE *Lab* space allows one to reveal their intrinsic features of curvature and torsion. These features are applied to define the ink limits in ink-jet printing systems and to create the empirical approach based on trajectories' curvature and torsion behavior analysis.

Such an approach might be expanded onto the grey balance management. It is known that the digital printing system performance might be greatly improved and the requirements on number of color measurements per calibration initialization might be greatly reduced when using the grey balance control systems [12]. Moreover, grey balance has been widely used in the sheet-fed offset [13] and web-offset printing [14] themselves, as well as in application of a digital printing press for simulating the offset printing [15]. Normally, the grey balance may be accounted in the Grey Component Replacement (GCR) procedure in a Color Management System (CMS) [16]. Sometimes, CMY-K balance is affected by spectral response properties of inks [17]. Despite the fact that calibrated

printing devices possess smooth and gradual changed tone curves and correct grey balance, they have their own characteristics in output color gamut with various saturation performances in every hue sections [18] that must be taken into account when adjusting the color. Another significant point in the grey balance is influence of chromaticity deviation of printing substrate that might be vital [19].

Methods of grey balance implication can vary in color management. The G7 specification by Idealliance consortium offers a simple methodology for the grey balance even for ink-jet [20]. Recent works have drawn more complicated math apparatus to establish a connection between CIE *Lab* and CMY-K colorants in order to manage the gray balance, e.g. polynomial regression [21] and artificial neural networks [22].

These approaches are based on certain model representations. In addition, the results obtained depend on the print type for which the assessment was carried out. Tradition of the gradation curves application in the characterization of printing devices led to widespread use of indirect (transformed) data in the calculations. The CIE *Lab* coordinates are not fully utilized, but only for determining the color difference. Till now, there has not been proposed an invariant model that would describe the gray balance for any printing method with sufficient accuracy.

This work is devoted to application of the gradation trajectories method for grey balance adjusting. We suggest using the Maxwell's Color Triangle as a basement of the model. We offer an empirical approach for a characterization, which implies a small number of prints and rapid calculations.

2 Approach

The Maxwell's Color Triangle relies on the Grassmann's law, which is an empirical result about human color perception that chromatic sensation can be described in terms of an effective stimulus consisting of linear combinations of different light colors. It works for additive color synthesis only. The major feature of the triangle is the following: by combining equal parts of basic colors, the neutral grey being obtained. Based on various print standards, it can be argued that this rule does not work for the process colors (CMY). In the case of printing colorants (CMY), their paired double overlays (binaries) correspond to additive primary colors (RGB). Since RGB and CMYK spaces are both device-dependent models, there has been no simple or general conversion formula that converts between them, as concerning the gray balance, at least. We might suggest the way to develop such a conversion based on the ideas of gradation trajectories and surfaces.

To start with, we have to outline a concept of gradation surfaces. The gradation trajectory of double overlays is a surface constructed on the basis of gradation trajectories of two colorants. Let us consider the formation of color with the participation of a certain type of substrate and 2 (two) colorants. Take as an example the pair of Cyan n and Magenta m inks. Each colorant is able to take a halftone value from 0 (pure substrate) to 1 (full dye). Thus,

$$\begin{array}{c} n \in [0;1] \text{ for Cyan}, \\ m \in [0;1] \text{ for Magenta}. \end{array} . \tag{1}$$

In the case of continuous halftones, we obtain a square region of allowable recipes on the plane (n, m). In real print, a frequent grid occurs instead of a solid square. Each reproducible tone has its own recipe (n, m) and a set of *Lab*-coordinates. A smooth change in tone causes a smooth change of *Lab*-coordinates. We can represent it in the form, which describe smooth surfaces in *Lab*-space,

$$a = a\ (n, m)\,;\ b = b\ (n, m)\,;\ L = L\ (n, m)\,. \tag{2}$$

Equation (2) seems to be equal to one of the surface in the Cartesian space [23]. Thus, a gradation surface is a locus of points in the *Lab*-space that satisfies the system of conditions (1) and (2). Heaving the printing system to be preliminary characterized, it might be assumed that gradation trajectories of a single color channel effectively described by polynomials of the degree not higher than third. For b and L coordinates, equations have the same type. Note a_0, b_0, L_0 as the coordinates of the substrate

$$\begin{array}{c} a_{\text{Cyan}} = a_0 + \sum_{i=1}^{3} a_{\text{Cyan},i} \bullet n^i, \\ a_{\text{Magenta}} = a_0 + \sum_{i=1}^{3} a_{\text{Magenta},i} \bullet m^i. \end{array} . \tag{3}$$

We designate a binary gradation surface as "stretched" on the gradation trajectories of generatrix pairs of colorants so that it contain them inside. In system (2), it will be reflected as special cases, as for instance, the gradation trajectory Cyan is contained in the gradation surface of Blue tones (4).

$$a = a\ (n, 0)\,;\ b = b\ (n, 0)\,;\ L = L\ (n, 0)\,. \tag{4}$$

When gradation surface is stretched on the gradation trajectories, then, taking into account (3), we can write the explicit form of (2) as (5). For b and L coordinates, equations have the same type

$$a_{\text{Blue}} = a_0 + \sum_{i=1}^{3} \sum_{j=0}^{i} a_{i-j,j} \bullet n^{i-j} \bullet m^j. \tag{5}$$

The required degree of the polynomial (third) was approved experimentally. The graph of the analytic surface (see Fig.1) is deviated from the experimental data by a distance smaller than the measurement error of the spectrophotometer. A polynomial of the third degree was quite accurate, so the fourth-degree polynomial was superfluous.

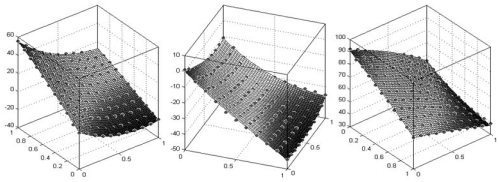

Fig. 1. Approximations of *Lab*-coordinates (2) by (5): left picture is for a, central picture is for b, right one is for L; dots are the measured values; halftones surfaces are approximations.

Further, we have to introduce a concept of geodesic lines. Characterization of a printing machine is made by a uniform distribution of points along the gradation curve. Therefore, it would be logical to assume that this principle should also be adhered to in the case of a double halftone surface. Since the figure of double superimposition in color space is not a curve, but a surface, the points should be located evenly within the surface i.e., at an equal distance from each other to be a grid. It is precisely this goal that an element of differential geometry, such as geodesic lines, perfectly fit. A geodesic line is an analog of a straight line on a plane for a surface, i.e., straight line, which, by the shortest path, connects two points on the surface. The basic property of a geodesic line is: on any sufficiently small piece of surface through two points the only one arc of the geodesic line can be drawn, just as on a plane through two points the only one straight line passed.

Below, we describe an algorithm for finding out a geodesic in general form. In our case, we consider a regular piece of the surface B (blue) defined by vector equations (2). The first fundamental form of the surface B is the following (6):

$$\begin{gathered} dB^2 = E\,(n,m)\,dn^2 + 2F\,(n,m)\,dndm + G\,(n,m)\,dm^2, \\ \text{where } E\,(n,m) = \left(\tfrac{da}{dn}\right)^2 + \left(\tfrac{db}{dn}\right)^2 + \left(\tfrac{dL}{dn}\right)^2, \\ F\,(n,m) = \tfrac{da}{dn}\tfrac{da}{dm} + \tfrac{db}{dn}\tfrac{db}{dm} + \tfrac{dL}{dn}\tfrac{dL}{dm}, \\ G\,(n,m) = \left(\tfrac{da}{dm}\right)^2 + \left(\tfrac{db}{dm}\right)^2 + \left(\tfrac{dL}{dm}\right)^2. \end{gathered} \quad . \tag{6}$$

A regular piece of the surface B with the first fundamental form is a two-dimensional Riemannian space referred to the coordinates (n, m). If we consider a surface as a Riemannian space, then vectors, tensors, scalar products, and covariant differentiation can be defined on it [24]. The three-index Christoffel symbols have the following form for the surface B:

$$\begin{gathered} \Gamma^1_{11} = \left\{ \begin{array}{c} 1 \\ 1\,1 \end{array} \right\}_B = \tfrac{GE_n - 2FF_n + FE_m}{2(EG - F^2)}\ , \Gamma^2_{11} = \left\{ \begin{array}{c} 2 \\ 1\,1 \end{array} \right\}_B = \tfrac{-FE_n + 2EF_n - EE_m}{2(EG - F^2)}, \\ \Gamma^1_{12} = \left\{ \begin{array}{c} 1 \\ 1\,2 \end{array} \right\}_B = \left\{ \begin{array}{c} 1 \\ 2\,1 \end{array} \right\}_B = \tfrac{GE_n - FG_m}{2(EG - F^2)},\ \Gamma^2_{12} = \left\{ \begin{array}{c} 2 \\ 1\,2 \end{array} \right\}_B = \left\{ \begin{array}{c} 2 \\ 2\,1 \end{array} \right\}_B = \tfrac{EG_n - FE_m}{2(EG - F^2)},\ . \\ \Gamma^1_{22} = \left\{ \begin{array}{c} 1 \\ 2\,2 \end{array} \right\}_B = \tfrac{-FG_m - 2GF_m - GG_n}{2(EG - F^2)}, \Gamma^2_{22} = \left\{ \begin{array}{c} 2 \\ 2\,2 \end{array} \right\}_B = \tfrac{EG_m - 2FF_m - FG_n}{2(EG - F^2)}\,. \end{gathered} \tag{7}$$

For any geodesic $m = m(n)$, the corresponding function $m(n)$ satisfies the differential equation

$$\frac{d^2m}{dn^2} = \Gamma^1_{22\,B}\left(\frac{dm}{dn}\right)^3 + \left[2\Gamma^1_{12\,B} - \Gamma^2_{22\,B}\right]\left(\frac{dm}{dn}\right)^2 + \left[\Gamma^1_{11\,B} - 2\,\Gamma^2_{12\,B}\right]\frac{dm}{dn} - \Gamma^2_{11\,B}. \tag{8}$$

The gradation trajectory of the Blue color is the curve in the *Lab*-space containing two points (n,m)=(0,0) as pure substrate and (n,m)=(1,1) as binary dye. Moreover, this curve must lie on the surface of blue halftones B. Thus, the gradation trajectory of the Blue color is the geodesic satisfying equation (8) with boundary conditions $m(0)$=0, $m(1)$=1 (Fig.2). The gradation trajectory of the

Blue color obtained by this manner does not meet the traditional representation of equal recipes everywhere except full dye. Such an approach ensures the invariance of the hue in the entire range of gradations of the Blue color.

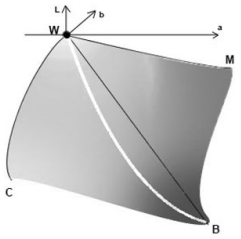

Fig. 2. The gradation surface of the Blue (B) halftones stretched on gradation trajectories of cyan and magenta (CM); white curve is a geodesic; black line is a nominal line of the Blue color by recipe $C{=}M$; W is a white point (substrate).

We can carry out similar calculations for the Red and Green colors that are corresponding binaries of Magenta-Yellow (M-Y) and Yellow-Cyan (Y-C), respectively.

For convenience of the following writing, we replace the notation. Instead of the variables m, n (1), we will use the corresponding letter to denote the relative proportion of the ink. Then, the obtained geodesic equations corresponding to the Red (R), Green (G), and Blue (B) colors, respectively, will take the form

$$1.\ Y = \varphi_R\,(M)\,.\ 2.\ Y = \varphi_G\,(C)\,.\ 3.\ M = \varphi_B\,(C)\,. \tag{9}$$

The following order of mutual dependence of variables is accepted: the variable placed earlier in abbreviation CMY will be considered independent. Therefore, the variable C is always independent, and Y is always dependent. M (magenta) is considered independent in the calculation of the Red geodesic, and acts as dependent when calculating the Blue one. Dependences (9) are effectively described by polynomials of the third degree.

After obtaining analytical dependencies (9), the values of neutral gray tone formulations are formed from the values taken at a level of the equal lightness ($L_R{=}L_G{=}L_B$). The formulations of the necessary primary dyes are calculated by formulas (10), where the values in square brackets "[...]" indicate the corresponding equation from (9)

$$C = \frac{C\,[9.2] + C[9.3]}{2};\ M = \frac{M\,[9.1] + M[9.3]}{2};\ Y = \frac{Y\,[9.1] + Y[9.2]}{2}. \tag{10}$$

The empirical approach that we describe is the following. Preliminary linearization → Print specially developed test chart → Measure *Lab* coordinates of the chart with a spectrophotometer → Sorting data by color channels in order to extract R,G,B tone surfaces → Fit surfaces fitting by a polynomial of third degree (3)–(5) → Calculate of the geodesics from 0 to the full dye for R,G,B tones

→ Use geodesics obtained as arguments for (2) → Define equal lightness levels → Calculate the grey balance formulations by (10) → Print test chart to assess the result. All our models are built with help of the MatLab package.

3 Experimental

For the experiment, we use the 4-color (CMYK) wide-format solvent ink-jet printer Mimaki CJV30-160BS. Print mode: 720×720 dpi, small dot. Substrate: coated paper FancyEmboss 110 g/m^2 as an absorbent substrate. The measurement tools: spectrophotometer x-Rite iOne iSis + x-Rite ProfileMaker package.

A halftone scale contains 14800 fields. The scale represents the multidimensional grid of test values. The total number of patches is 11 (0, 0.1, 0.2...1) values per channel to the power of the number of colorants (four). They are synthesized using the Argyll CMS and TestChartGenerator in ProfileMaker for the automatic iOne iSis spectrofotometer. Such a frequent grid allow one to distinguish all possible surfaces within the device's color space. We utilized surfaces of binaries only, *i.e.*, it formed 121 patch per each surface. Thus, 330 patches were actually used. Matrix variables, which contained n, m, L, a, and b data of each color patch as columns, are imported in MatLab, where they are carried out in further mathematical processing.

The proposed method of gradation surfaces is based on the interpolation of experimental data by polynomials (5). The approximation of dependences (2) by polynomials (5) is implemented in MatLab package using the fit function. Final evaluation is done by preparation of a new arbitrary scale that is further printed out and measured (see Fig. 3b).

4 Results and discussion

Results of geodesics calculations by (9) are shown in Table 1. Evidently, gradations of the Red, Green, and Blue tones do not match equal recipes of process inks. Figure 3a shows the dependencies of lightness (CIE L) on the part of tone for independent variables: Magenta for Red, Cyan for Green, and Cyan for Blue. Trends in the Figure show the linear dependency that confirm the printing system linearity. Moreover, such linearity is convenient for definition of equal lightness levels.

The maximum possible value of the neutral color recipe (without the involvement of K-black) is determined by the component that has the highest brightness of the full tone (red). The errors in terms of deviations from the linear trends we associate with the rounding error, because it is impossible to put the formulation into the source code with a precision of better than a few percent. The developed and printed test chart for grey balance evaluation is shown in Fig. 3b.

Table 1. Calculated geodesics

R		G		B	
Magenta	Yellow	Cyan	Yellow	Cyan	Magenta
0.00	0.00	0.00	0.00	0.00	0.00
0.05	0.06	0.05	0.04	0.05	0.05
0.10	0.11	0.10	0.07	0.10	0.11
0.15	0.17	0.15	0.11	0.15	0.16
0.20	0.22	0.20	0.15	0.20	0.22
0.25	0.28	0.25	0.19	0.25	0.28
0.30	0.33	0.30	0.23	0.30	0.34
0.35	0.38	0.35	0.27	0.35	0.40
0.40	0.43	0.40	0.31	0.40	0.46
0.45	0.48	0.45	0.36	0.45	0.53
0.50	0.53	0.50	0.41	0.50	0.59
0.55	0.58	0.55	0.46	0.55	0.65
0.60	0.63	0.60	0.51	0.60	0.71
0.65	0.68	0.65	0.57	0.65	0.77
0.70	0.72	0.70	0.62	0.70	0.82
0.75	0.77	0.75	0.68	0.75	0.87
0.80	0.82	0.80	0.75	0.80	0.91
0.85	0.86	0.85	0.81	0.85	0.94
0.90	0.91	0.90	0.87	0.90	0.96
0.95	0.95	0.95	0.93	0.95	0.99
1.00	1.00	1.00	1.00	1.00	1.00

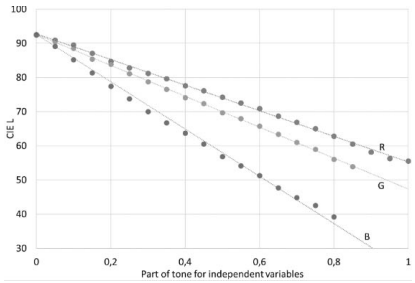

a

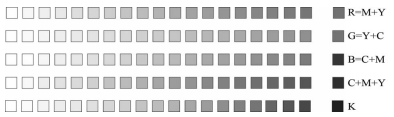

b

Fig. 3. Dependencies a) of lightness (CIE L) on the part of tone; b) test chart for GB evaluation

Figure 4 shows the lines of red, green, and blue tones in the CIE *Lab* space and a line of synthesized neutral colors.

Analysis of the nature of deviation of chromaticity from the neutral tone indicates the accumulation of a systematic error. This is probably due to inadequate accuracy of the condition of equal lightness when the tone of red, green, and blue increases. Nevertheless, as it can be seen from Fig.5, the line of neutral colors is close to the vertical.

For convenience, we show the projections of points of the neutral tone on the chromaticity plane, which are grouped near zero, with the exception of the latter. A visual comparison of synthesized neutral fields with blacks matched in brightness (K) has shown an interesting phenomenon. It is impossible to determine, which field is composite, and what is black, in spite of some difference in the shades.

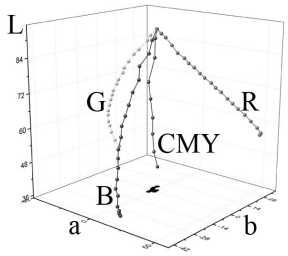

Fig. 4. Trajectories of R,G,B tones and the neutral grey with its projection at *ab* field

5 Conclusion

A new three-dimensional interpretation of the grey balance and application of gradation curves in 3D CIE *Lab*-space for the grey balance evaluation are proposed for up-to-date digital image processing. Gradation trajectories in terms of gradation surfaces, as well as the method of their analytical specification, are described. Gradational trajectories are conceived as continuous and bounded on the gradation range curves where the gradation surfaces are stretched on.

Gradation trajectories introduced by the described manner are the global features of ink-jet image processing that are depended only on type of a substrate and properties of the ink. They are not affected by rasterizing method, number of passes, and measuring technique.

Grey balance evaluation with the help of the gradation trajectories of inks binaries (R, G, B) instead of inks themselves (C, M, Y) might be utilized as a powerful and fast-acting tool for printing systems characterization.

Further development of the approach implies introduction of 3D gradation surfaces as a method describing interconnection between two or even three colorants, especially in the case of regular and light inks pairs and not only for ink-jet, but, also, for all kinds of print.

References

1. Bala, R.: Device characterization. Digital Color Imaging Handbook. G. Sharma (ed.). CRC Press, Boca Raton, FL, 269–379 (2003)
2. Balasubramanian, R.: Optimization of the spectral Neugebauer model for printer characterization. J Elec.Imag. 8, 156–166 (1999)
3. Hersch, R.D., Crété, F.: Improving the Yule–Nielsen modified spectral Neugebauer model by dot surface coverages depending on the ink superposition conditions. Proc. SPIE 5667, 434–445 (2005)
4. Wyble, D.R., Berns, R.S.: A critical review of spectral models applied to binary color printing. Col.Res.&App. 25, 4–19 (2000)

5. Garg, N.P., Singla, A.K., Hersch R.D.: Calibrating the Yule–Nielsen Modified Spectral Neugebauer Model with Ink Spreading Curves Derived from Digitized RGB Calibration Patch Images. J.Imag.Sci.Tech. 52(4), 040908–040908-5 (2008)
6. Arney, J.S., Engeldrum, P.G., Zeng H.: An expanded Murray-Davis model of tone reproduction in halftone imaging. J.Imag.Sci.Tech. 39, 502–508 (1995)
7. Livens, S.: Optimisation of Printer Calibration in the Case of Multi Density Inks. Conference on Color in Graphics, Imaging, and Vision, CGIV 2002. Final Program and Proceedings, 633–638 (2002)
8. Chagas, L., Blayo, A., Giraud P.: Color Profile: methodology and influence on the performance of ink-jet color reproduction. IS&T's NIP20. 2004 International Conference on Digital Printing Technologies, 655–659 (2004)
9. Wu, Y-J.: Reducing Ink-jet Ink Consumption with RIP software for POP Display Media. Digital Fabrication and Digital Printing. NIP30 Technical Program and Proceedings, 108–111 (2014)
10. Kipphan, H.: Handbook of Print Media. Springer-Verlag Berlin-Heidelberg. 1207p. (2001)
11. Milder, O.B., Tarasov, D.A., Titova, M.Yu.: Inkjet Printers Linearization Using 3D Gradation Curves. CEUR Workshop Proceedings. 1814. Proceedings of the 1st International Workshop on Radio Electronics & Information Technologies (REIT 2017), 74–83 (2017)
12. Mestha, L.K., Viturro, R.E., Wang, Y.R., Dianat, S.A.: Grey Balance Control Loop for Digital Color Printing Systems. NIP & Digital Fabrication Conference, 2005 International Conference on Digital Printing Technologies. 499–504(6) (2005)
13. Enoksson, E., Ullberg, J.: Grey balance control in sheet-fed offset printing. Proceedings of the Technical Association of the Graphic Arts, TAGA, 153–176 (2008)
14. Zhu, Y.S., Xu, X.Y., Wang, L.J.: The characterization of web offset equipment based on the measurement of chromaticity. Adv.Mat.Res. 718–720, 923–927 (2013)
15. Xu, Y., Jiang, G., Wang, L., Liu, H.: Study on color simulating between offset printing and digital printing. Adv.Mat.Res. 174, 235–238 (2011)
16. Spiridonov, I., Shopova, M., Boeva, R.: Study of the effect of grey component replacement level on reflectance spectra and color reproduction accuracy. Proceedings of SPIE. 8770, 87700W (2013)
17. Zhu, M., Chen, Z., Liu, H.: The research on special printing effects based on Grey Component Replacement. Adv.Mat.Res. 174, 251–254 (2010)
18. Xu, Y., Nan, L., Guo, G., Jiang, G.: Analysis of color performance of digital output devices. Proceedings - 4th International Congress on Image and Signal Processing. 4, 6100542, 1737–1740 (2011)
19. Huan-Me, W., Guang-Xue, C., Xiao-Meng, C.: Effect on grey balance caused by slight chromaticity deviation of paper in image reproduction. App.Mech.Mat. 236-237, 459–463 (2012)
20. Wang, Z.R., Tang, W.Y.: Research on the gray balance of ink-jet printing based on G7. App.Mech.Mat. 329, 429–433 (2013)
21. Sun, B.Y., Zhou, S.S., Cao, C.J., Zheng, Y.L.: A method of obtaining gray balance data based on polynomial regression. Adv.Mat.Res. 213, 643–646 (2011)
22. Zhao, C.: Prediction of gray balance spectral data in digital printing. LecNotElecEng. 369, 111–116 (2016)
23. Pogorelov, A.V.: Differential geometry. Noordhoff, 171pp. (Transl. from Russian) (1959)
24. Korn, G.A., Korn, T.M.: Mathematical Handbook for Scientists and Engineers: Definitions, Theorems, and Formulas for Reference and Review. Courier Corporation, 1130p. (2000)